Clim Dyn (2014) 43:259–270
DOI 10.1007/s00382-013-1928-0

Upper tropospheric warming intensifies sea surface warming

Baoqiang Xiang · Bin Wang · Axel Lauer · June-Yi Lee · Qinghua Ding

Received: 28 February 2013 / Accepted: 20 August 2013 / Published online: 30 August 2013

Abstract One of the robust features in the future projections made by the state-of-the-art climate models is that the highest warming rate occurs in the upper-troposphere especially in the tropics. It has been suggested that more warming in the upper-troposphere than the lower-troposphere should exert a dampening effect on the sea surface warming associated with the negative lapse rate feedback. This study, however, demonstrates that the tropical upper-tropospheric warming (UTW) tends to trap more moisture in the lower troposphere and weaken the surface wind speed, both contributing to reduce the upward surface latent heat flux so as to trigger the initial sea surface warming. We refer to this as a 'top-down' warming mechanism. The rise of tropospheric moisture together with the positive water vapor feedback enhance the downward longwave radiation to the surface and facilitate strengthening the initial sea surface warming. Meanwhile, the rise of sea surface temperature (SST) can feed back to intensify the initial UTW through the moist adiabatic adjustment, completing a positive UTW–SST warming feedback. The proposed 'top-down' warming mechanism and the associated positive UTW–SST warming feedback together affect the surface global warming rate and also have important implications for understanding the past and future changes of precipitation, clouds and atmospheric circulations.

B. Xiang (✉) · B. Wang · A. Lauer
International Pacific Research Center, School of Ocean and Earth Science and Technology, University of Hawaii, Honolulu, HI 96822, USA
e-mail: baoqiang@hawaii.edu

B. Wang
Department of Meteorology, School of Ocean and Earth Science and Technology, University of Hawaii, Honolulu, HI 96822, USA

Present Address:
A. Lauer
Institute for Advanced Sustainability Studies, Potsdam, Germany

J.-Y. Lee
Institute of Environmental Studies, Pusan National University, Busan, Korea

Q. Ding
Department of Earth and Space Sciences, Quaternary Research Center, University of Washington, Seattle, WA, USA

1 Introduction

The global mean temperature has been experiencing a conspicuous warming since the last century especially during the period after 1950s. The observed warmer climate has caused more frequent occurrences of severe weather and extreme climate worldwide (e.g., Easterling et al. 2000). As is well known, the observed surface temperature is tightly linked to some external forcing. In particular, the steadily increase of carbon dioxide (CO_2) and other greenhouse gases (GHGs) is largely responsible for the observed surface warming (Meehl et al. 2007). In addition, the increased solar irradiance was also suggested to strengthen the surface warming rate on a longer time scale since the Little Ice Age (Liu et al. 2013), but its relative contribution to the recent observational warming rate remains unclear.

Besides the direct forcing effect associated with GHGs and solar forcing, various climate-feedbacks have been shown to play a pivotal role in determining the surface warming rate by amplifying or reducing the radiative forcing effect (Bony et al. 2006; Mitchell 1983; Soden and Held 2006). An important feedback is the lapse rate feedback, which is thought to exert a dampening effect on the

surface warming because more warming in the upper-troposphere tends to radiate more energy to space compared to a uniform temperature change (Bony et al. 2006; Soden and Held 2006). Although there are large disagreements and uncertainties for different observations in terms of the lower- and upper-tropospheric temperature change rate (Fu et al. 2011; Santer et al. 2008), the highest warming occurring in the tropical upper-troposphere is a very robust feature with respect to the future climate projections from the state-of-the-art climate models that participated in the Coupled Model Intercomparison Project (CMIP) phase 3 (CMIP3) (Solomon 2007) and phase 5 (CMIP5) (Taylor et al. 2011) (Fig. 1a).

Then, what is responsible for the upper-tropospheric warming (UTW)? The atmospheric response to external forcing (e.g., GHGs or solar forcing) can be roughly separated into a rapid response and a slow response (Bala et al. 2010; Gregory and Forster 2008). The UTW is related to both of these two processes. The slow response depends on changes in sea surface temperature (SST) and the fast process typically refers to the atmospheric adjustment before the ocean responds to the atmospheric warming. There is a broad consensus that the UTW is largely determined by the slow process following the boundary SST changes confirmed by the strong correlation between the UTW and SST changes from the multi-model ensemble of CMIP3 (Johnson and Xie 2010) and CMIP5 models (Fig. 2). The SST-induced UTW is caused by an intensified convection and the moist adiabatic adjustment (Knutson and Manabe 1995; Manabe et al. 1965), which can result in the vertical differential warming rate especially over the tropical regions (Johnson and Xie 2010; Knutson and Manabe 1995; Richter and Xie 2008). The fast atmospheric response to external forcing can also lead to a rapid UTW. Based on model results, Cao et al. (2012) illustrated that the increase of solar forcing can induce more warming in the upper-troposphere than the lower-troposphere within 1 month. In this study, we demonstrate that the fast atmospheric response to an instantaneous increase of the CO_2 concentration also results in a maximum warming rate in the tropical upper-troposphere.

The central goal of this study is to address the possible impact of the fast UTW related to GHGs or solar forcing on the SST warming rate. Previous studies suggested that the UTW can influence the atmospheric circulation, hydrological cycle and may further exert an indirect role in altering the SST. For example, the UTW was suggested to weaken the atmospheric circulation (Ma et al. 2011), widen the Hadley circulation (Frierson et al. 2007; Lu et al. 2007; Wang et al. 2012) and shift the mid-latitude storm tracks poleward (Butler et al. 2010; Schneider et al. 2010; Wang et al. 2012; Yin 2005); The UTW can increase atmospheric stability (Lee and Wang 2013; Ma et al. 2011), increase the threshold for deep convection (Johnson and Xie 2010) and thus suppress precipitation (Richter and Xie 2008); The UTW may also influence the energy balance of the Earth's climate system by changing water vapor and clouds (Colman 2001). In this study, we investigate the potential role of the UTW on the SST changes based on climate model results with an imposed upper-tropospheric heating.

This paper is organized as follows. Section 2 describes the models and experiments used in this study. Section 3 examines the atmospheric fast response to the GHGs forcing. The following Sect. 4 discusses how the UTW

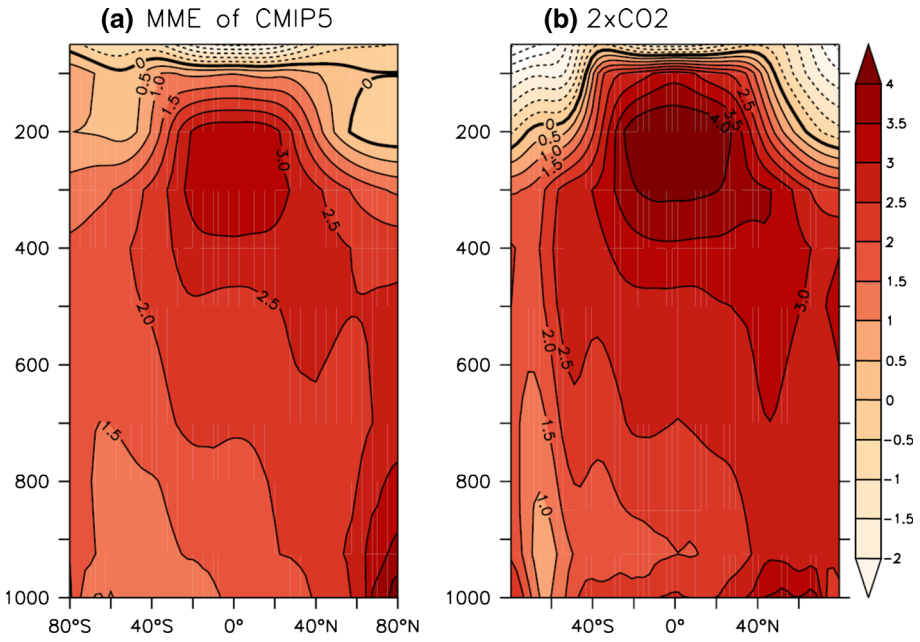

Fig. 1 **a** Multi model ensemble mean (MME) of zonally averaged temperature changes between the RCP 4.5 simulation for the period 2071–2100 and the historical simulation for the period 1980–2005. Zonally averaged temperature (°C) changes in response to **b** double CO_2 (C-2CO_2 − C-CTRL) based on the POEM coupled model

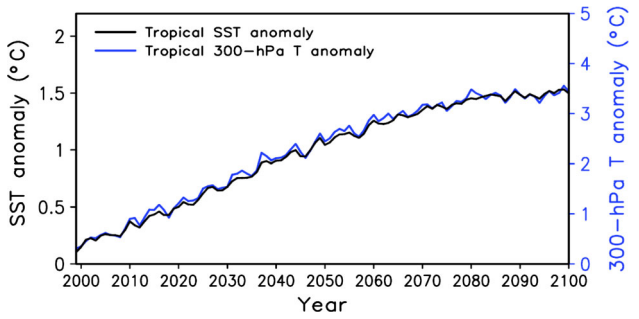

Fig. 2 Time evolutions of the SST and 300-hPa temperature anomalies over the Tropics (30°S–30°N) obtained from the 20 model multi-model ensemble mean (MME) for the RCP4.5 run. Anomalies are relative to the 1980–2005 climatology from the historical run. The *left y-axis* corresponds to the tropical mean SST anomaly, the *right y-axis* corresponds to the 300 hPa temperature anomaly

triggers and intensifies the sea surface warming. Finally we summarize the findings in this study and its potential implications.

2 Models and experiments

In order to assess how the UTW influences the surface temperature changes, we perform numerical experiments with an atmospheric general circulation model (AGCM) and a coupled general circulation model (CGCM). The AGCM is the ECHAM (v4.6) model (Roeckner 1996). Here we use T42 horizontal resolution with 19 sigma levels in the vertical extending from the surface to 10 hPa. The CGCM is a newly developed atmosphere–ocean coupled model named POP–OASIS–ECHAM model (POEM), which couples the POP (v2.0.1) ocean model and ECHAM (v4.6) atmospheric model through the OASIS coupler (v3.0) (Xiang et al. 2012). We use a relatively coarse resolution of ocean model with 100 (longitude) × 116 (latitude) grid point in the horizontal and 25 levels in the vertical. In the CGCM, the atmosphere is coupled to the ocean between 60°S and 60°N. A higher latitudes SST and sea ice are prescribed according to the observed climatology. We apply a SST correction scheme over the equatorial central Pacific and southeast Pacific to artificially eliminate the commonly seen, mean SST bias associated with the double Inter-tropical Convergence Zone (ITCZ) problem (Xiang and Wang 2013). The SST correction term is estimated by inversely fitting model SST tendency to observational climatology with the nudging method, and thus a long-term annual SST correction term can be obtained. The SST correction (nudging) term is exactly the same for all the coupled model experiments in this study. With the SST correction, the mean state of SST and precipitation is realistic compared with observations (Fig. 3). Given the fact that the maximum UTW is near the tropical region (Fig. 1), the current POEM coupled model is thus an appropriate tool to study the potential influence of UTW on surface temperature changes even without an interactive sea ice model component. This model has been used for several recent studies which show realistic performance of this CGCM (e.g., Wang et al. 2013; Xiang and Wang 2013).

Seven experiments are conducted with two control runs and four sensitivity experiments (Table 1). The first control run (C-CTRL) is a free running coupled experiment using the POEM coupled model (40-year). The parameter setting in the sensitivity experiments is the same as in C-CTRL except with prescribed abrupt double CO_2 concentrations (C-2CO_2) and an imposed upper-tropospheric heating (C-HEAT). The imposed idealized heating is in the upper-troposphere between 50 and 550 hPa with a maximum at 250 hPa, which is zonally uniform but varies in meridional direction (Fig. 4). The design of the heating pattern is based on the projected warming pattern (Fig. 1b) and also the fact that the UTW has weak zonal gradients because of fast wave adjustment in the tropics (Sobel et al. 2001; Xie et al. 2010). Similar to C-HEAT, another coupled experiment is performed with its maximum heating shifting to 30°S and 30°N while the heating rate is zero at the equator (C-HEAT-30). The data analyzed from the CGCM sensitivity experiments include only the last 20 years of the 50-year integrations.

Similarly, we also carry out another control run (A-CTRL) by using the AGCM (atmosphere-only) with

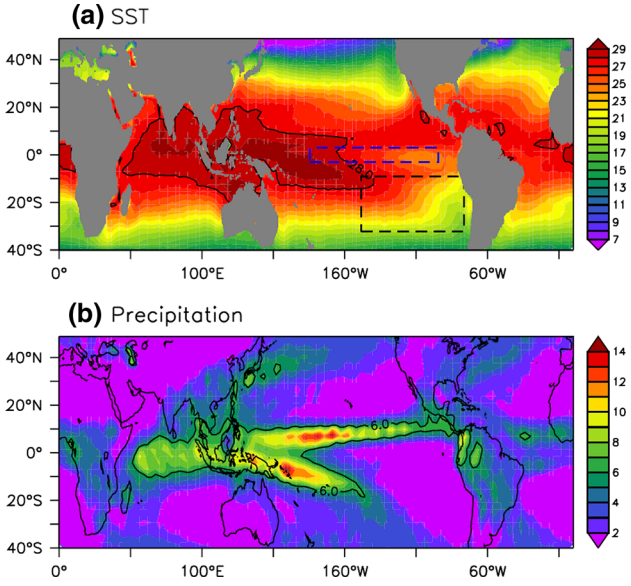

Fig. 3 Annual mean **a** SST (°C) and **b** precipitation (mm/day) from the control run of POEM coupled model (C-CTRL). A SST correct scheme is used over the equatorial Pacific (*blue box* in **a**) and southeastern Pacific (*black box* in **a**) to eliminate the mean SST bias

Table 1 List of model experiments in this study

Experiments	Description
C-CTRL	Control run of the coupled model (POEM) (40-year)
C-2CO_2	Coupled model run with abrupt double CO_2 (50-year)
C-HEAT	Coupled model run with prescribed upper-tropospheric heating (Fig. 4) (50-year). 5 ensembles are performed for the first 5 years to examine the evolution features associated with upper-tropospheric heating
C-HEAT-30	Same as C-HEAT but with the maximum heating shifting to 30°S and 30°N. The heating rate is zero at the equator (Fig. 13a)
A-CTRL	AGCM control run with prescribed climatological SST and sea ice
A-2CO_2	AGCM run with abrupt double CO_2 (10-year). 10 ensembles are used for the first month to show the transient atmospheric responses
A-HEAT	AGCM run with prescribed upper-tropospheric heating (Fig. 4) (10-year)

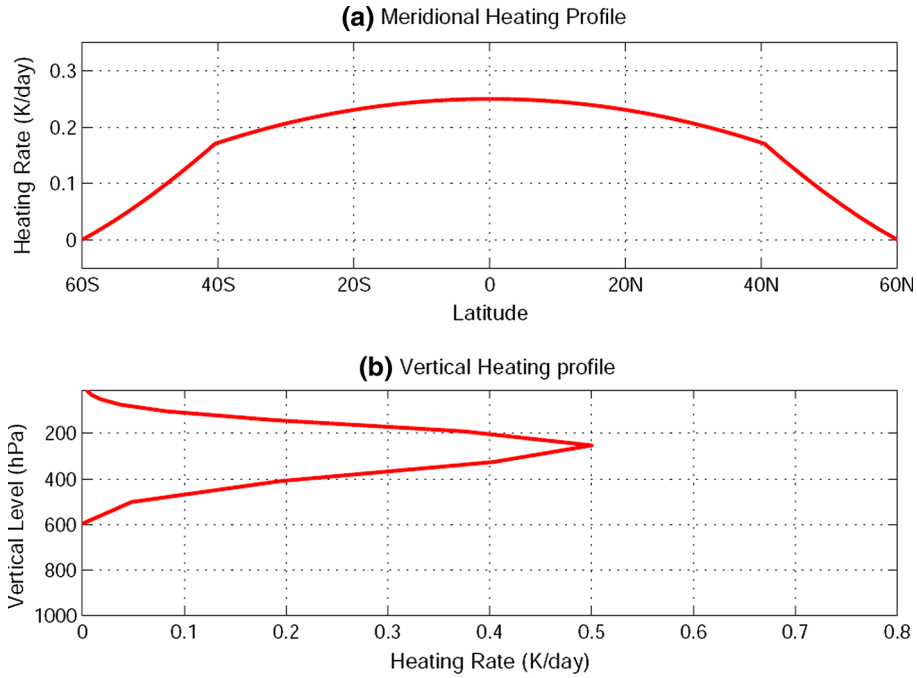

Fig. 4 **a** Meridional and **b** vertical heating profile from the C-HEAT and A-HEAT experiments. The prescribed heating profile is zonally uniform

prescribed climatological SST and sea ice forcing. Two AGCM sensitivity experiments (A-2CO_2, A-HEAT) are performed, which have the same atmospheric setup as the corresponding CGCM experiments. These AMIP type experiments are integrated for 10 years each.

In this study, we use 20 climate models that participated in CMIP5 (Taylor et al. 2011) in this study (Table 1 in Lee and Wang 2013). The projected future changes are estimated based on the RCP4.5 simulations for the period 2071–2100 relative to the corresponding historical simulations for the period 1980–2005.

3 Atmosphere fast adjustment to double CO_2 forcing

As mentioned above, the motivation of this study is to explore whether the fast atmospheric response associated with GHGs or solar forcing can feed back to influence the SST. First, we examine the rapid adjustment of the atmosphere with the double CO_2 forcing by performing the AGCM experiments (Table 1). This issue has been extensively studied by some recent studies (Andrews et al. 2009; Bala et al. 2010; Cao et al. 2012; Dong et al. 2009; Gregory and Forster 2008; Kamae and Watanabe 2012) from a global mean perspective, but here we are only focusing on the regions near tropics (30°S–30°N). 10 ensemble runs are used for both the control and double CO_2 experiments. Each ensemble is started from January 1st and here we do not consider the potential influence of seasonality.

Over the land areas, the lower-troposphere shows more warming in the first week and even on longer time scales (Fig. 5a). The land surface warming is attributed to reduced evaporation, and increased downward longwave and shortwave radiation (Cao et al. 2012; Dong et al. 2009; Kamae and Watanabe 2012). Over the tropical ocean regions, more warming is seen in the lower-troposphere in

the first week (Fig. 5b) because of the maximum instantaneous longwave radiative heating (Collins et al. 2006; Kamae and Watanabe 2012). However, on the time scales beyond 1 week, the upper-troposphere displays a much higher warming than the lower-troposphere. The vertical difference in the warming rate is expected to be governed by the moist adiabatic adjustment through convection (Knutson and Manabe 1995; Manabe et al. 1965). A notable cooling is evident in the stratosphere which can be ascribed to radiative origin (Hansen et al. 1997). This long-term mean (beyond one weak) of vertical temperature profile over ocean is somewhat different from other studies (Cao et al. 2012; Dong et al. 2009). We argue that the discrepancy may originate from the studied regions. We are considering the tropical regions with strong mean convection, and the moist adiabatic adjustment is more effective in driving the UTW over the tropics than other regions. Similar to the effect due to the solar forcing (Cao et al. 2012), the initial UTW can also be regarded as a fast response of the atmosphere to the enhanced GHGs concentrations. In the next section, we use AGCM and CGCM experiments to unveil the physical mechanisms of how the UTW alters the SST.

4 The SST changes due to upper-tropospheric heating forcing

Due to the complexity of air–sea interactions and climate feedbacks, it is difficult to identify the relative contributions of the UTW on the SST changes from other processes by using the conventional model experiments. Here we prescribe an idealized heating in the upper-troposphere (Fig. 4) in the POEM CGCM model and integrate 50 years. The POEM model then produces a pronounced sea surface warming related to the upper-tropospheric heating relative to the C-CTRL run (Fig. 6a). This warming pattern is strikingly similar to that obtained from the 'double CO_2' experiment (Fig. 6b) with a spatial correlation coefficient of 0.82. The gross feature of the sea surface warming pattern also bears close resemblance with the multi-model ensemble mean (MME) of the CMIP5 model results for the RCP4.5 scenario in the late twenty-first century (Fig. 6c). Similar to the double CO_2 forcing, it is expected that the UTW-induced sea surface warming is also prominently modulated by climatological mean surface winds and evaporation (Xie et al. 2010) so that more (less) warming occurs over the tropical (subtropical) oceans. Above comparisons indicate that the SST warming due to GHGs forcing may be partly ascribed to the UTW, and we refer to this SST warming caused by the UTW as a 'top-down' warming mechanism.

One more experiment has been carried out to test the sensitivity of the SST changes to the prescribed atmospheric heating forcing. The sensitivity experiment has the same horizontal heating pattern as in C-HEAT but shifts the maximum heating to the height of 500 hPa. It is noteworthy that this experiment generates a similar SST warming pattern as the one shown in Fig. 6a. This result is reasonable because the strong moist adiabatic adjustment favors the maximum warming occurring in the upper-troposphere even with the heating in the mid-troposphere.

The physical mechanisms of how the UTW causes the surface warming are not trivial because the complexity of

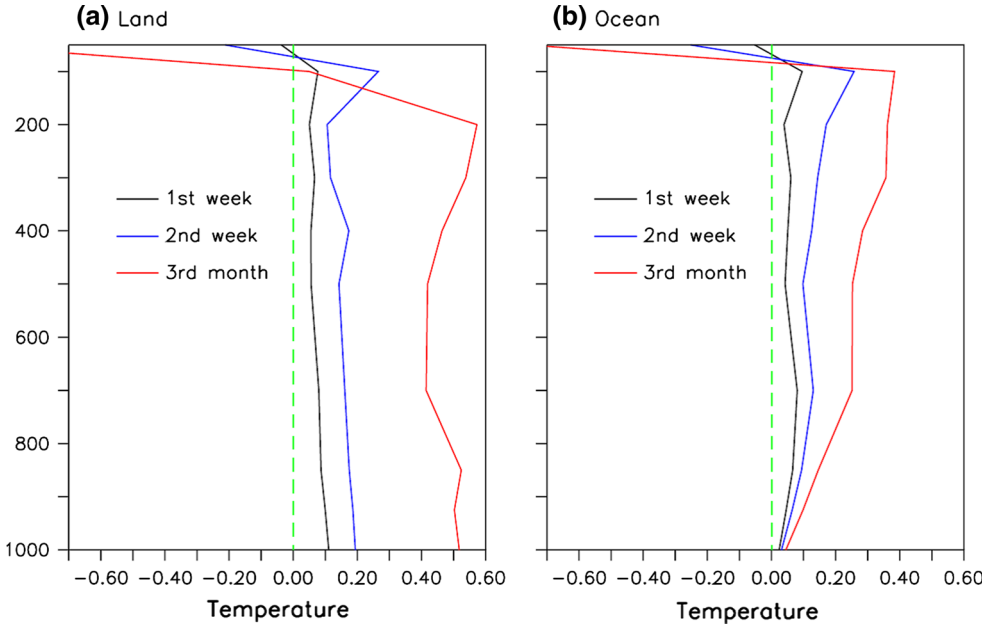

Fig. 5 Zonally (0°–360°) and meridionally (30°S–30°N) averaged temperature changes in the AGCM experiments associated with double CO_2 (A-2CO_2 − A-CTRL) for the first week (*black*), second week (*blue*) and the third month (*red*) over **a** land and **b** ocean

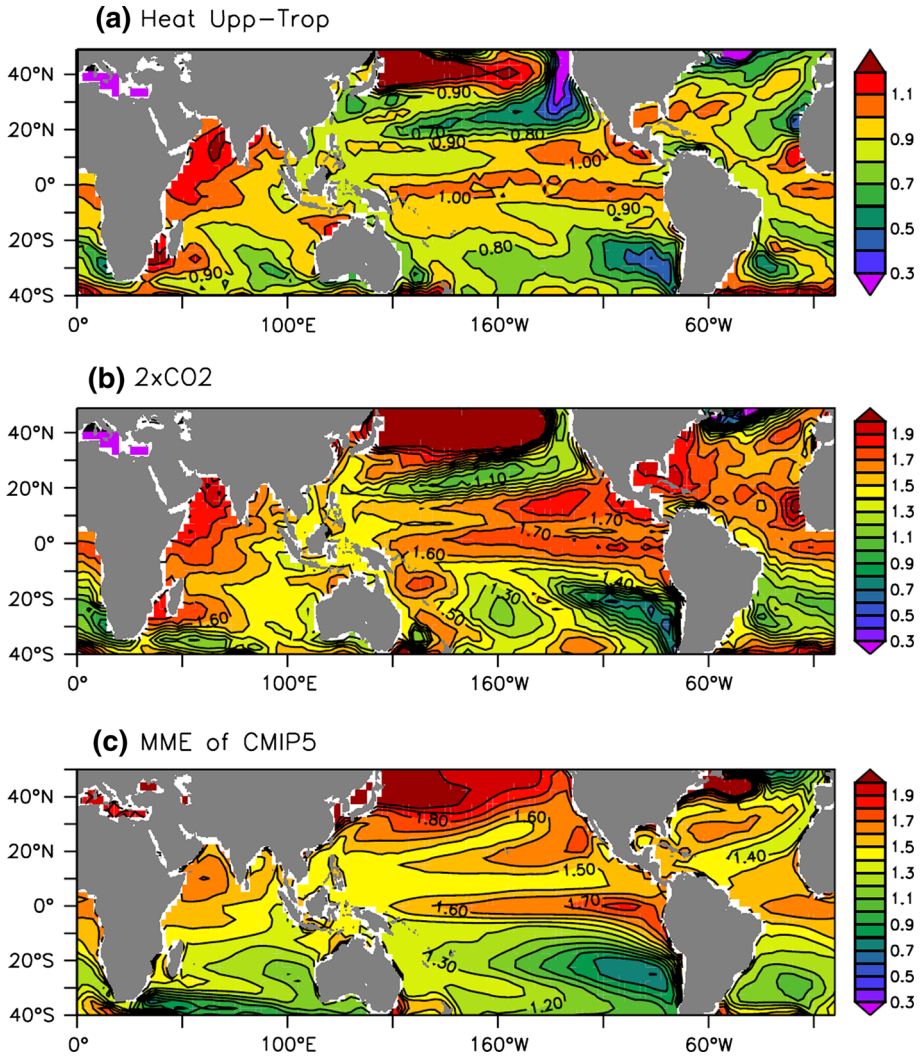

Fig. 6 SST changes in response to **a** prescribed heating in the upper-troposphere (C-HEAT − C-CTRL) and **b** double CO_2 (C-2CO_2 − C-CTRL) by using the POEM CGCM model. Shown are 20-year means from the last 20 years of 50-year integrations for the double CO_2 experiment and prescribed upper-tropospheric heating experiment. **c** Multi model ensemble mean (MME) of the SST changes between the RCP4.5 simulation for the period 2071–2100 and the historical simulation for the period 1980–2005 from the CMIP5 models

air–sea feedbacks makes it difficult to disentangle the underlying processes. However, the initial SST warming is to a certain degree forced by the atmosphere given the fact that the atmospheric response is much faster than the ocean. Therefore, in the following two subsections, we will address this issue by separating it into two questions by using AGCM and CGCM, respectively: (1) What processes trigger the initial sea surface warming associated with the upper-tropospheric heating? (2) Do and if so how do the air–sea interactions and feedbacks regulate the initial sea surface warming rate triggered by the upper-tropospheric heating?

4.1 How does the UTW trigger the initial sea surface warming?

In order to understand how the UTW triggers the initial sea surface warming, we examine the changes of the surface energy balance in response to the upper-tropospheric heating using the AGCM model with fixed SST and sea ice. The AGCM results largely represent the fast response of the atmosphere before the SST changes in a coupled system. We present, in Fig. 7, the surface heat flux changes related to the upper-tropospheric warming. Apparently, the upper-tropospheric heating induces a net downward surface heat flux in most oceanic regions (Fig. 7a). The changes in downward longwave radiation at the sea surface are small (Fig. 7d). The surface latent heat flux is positive (downward) in almost all ocean basins (Fig. 7c), and this effect is similar to the fast atmospheric response to an instantaneous increase in CO_2 in which case the boundary layer becomes warmer and moister (Andrews et al. 2009; Bala et al. 2010; Cao et al. 2012; Dong et al. 2009). The incoming shortwave radiation tends to partially counter-balance the downward latent heat flux in the tropics especially in regions with strong mean precipitation, but in the subtropics the shortwave radiation adds heat to ocean (Fig. 7b). As a consequence, the reduction of the upward latent heat flux acts as the key process bridging the UTW and the initial sea surface warming.

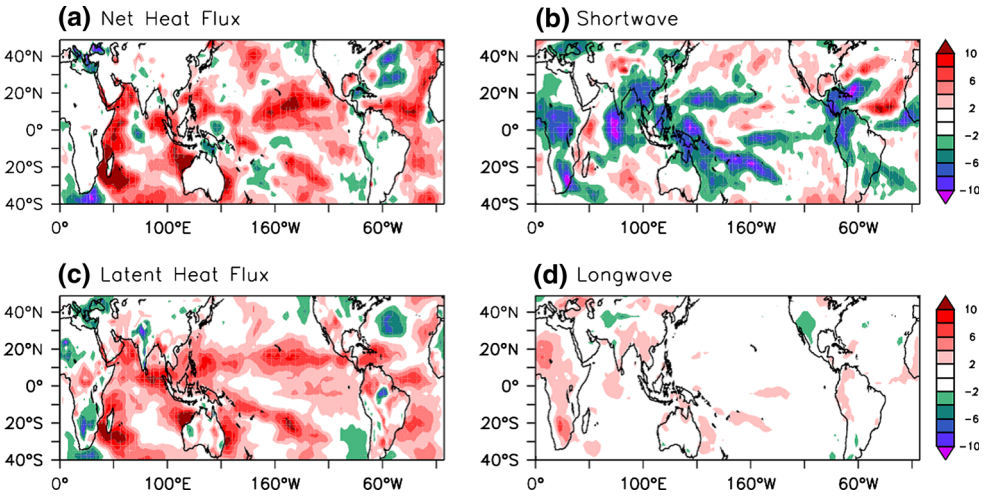

Fig. 7 Changes in the surface heat flux (W/m2) associated with the upper-tropospheric heating in the AGCM experiments (A-HEAT − A-CTRL). **a** Net heat flux; **b** shortwave radiation; **c** latent heat flux; and **d** longwave radiation. Positive means that ocean gets energy

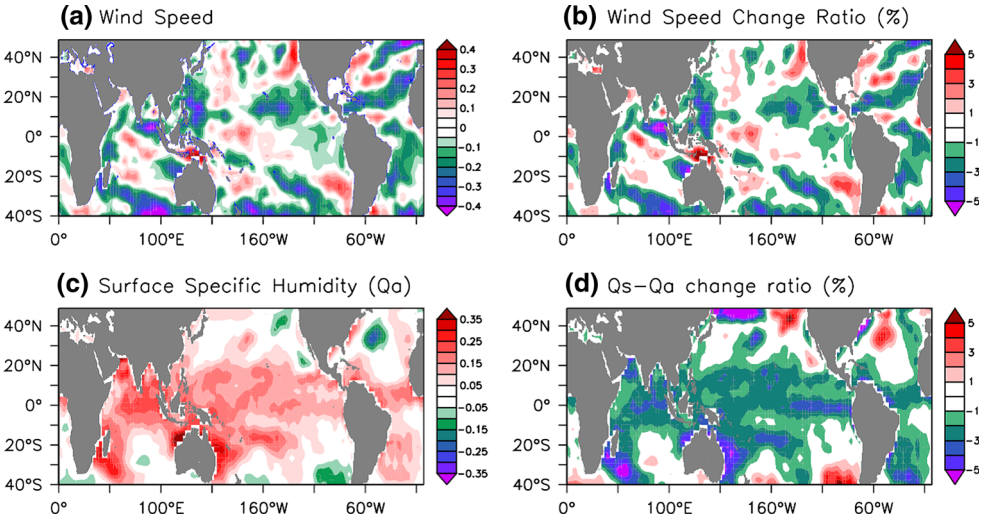

Fig. 8 Changes in **a** 1,000 hPa wind speed, and **b** its change ratio compared to the climatology (%) due to the upper-tropospheric heating in the AGCM experiments (A-HEAT − A-CTRL). **c**, **d** are the same as **a**, **b** but for 1,000 hPa specific humidity (g/kg) and the change ratio of Qs–Qa compared to the its climatology (%)

The reason for the reduced upward surface latent heat flux associated with the UTW requires a thorough investigation. With the fixed lower boundary forcing (SST and sea ice distribution), the changes of surface latent heat flux are dominantly controlled by the changes of surface wind speed and specific humidity (Qs–Qa) according to the standard bulk formula. Here Qs denotes the saturation specific humidity at the sea surface interface which depends on SST, and Qa represents the surface specific humidity. Note that the surface wind speed is calculated based on daily mean winds. Similar with the GHGs' effect (Held and Soden 2006; Richter and Xie 2008), the surface wind speed is weakened over most of the tropical oceans (Fig. 8a). The tropical (30°S–30°N) mean of wind speed is weakened by −0.7 % (0.05 m/s) over the ocean domains. Meanwhile, the surface specific humidity (Qa) is enhanced with a quite uniform spatial pattern (Fig. 8c), which is tightly linked to an increase in temperature (Fig. 9a) and an increase in relative humidity (∼0.5 %) (Fig. 10c). The resultant Qs-Qa is suppressed by −1.8 % over the tropical oceans (30°S–30°N) (Fig. 8d). Both the weakened surface wind speed and increased surface moisture contribute to the reduction of the upward latent heat flux whereas the latter dominates over the former.

More moisture trapped in the lower-troposphere is a key mechanism for the UTW to affect the SST. Two processes are responsible for the lower-tropospheric moisture changes associated with temperature and precipitation changes. First, the temperature rise (Fig. 9a) increases the water holding capacity in the lower troposphere, favoring the increase of surface specific humidity. Second, the stabilized atmosphere due to the UTW tends to weaken the deep convection as well as the vertical moisture transport so as to trap more moisture in the lower troposphere. Figure 11a shows a substantial reduction in precipitation over most ocean basins primarily due to the weakened convective precipitation. Physically, the reduced convective precipitation can be explained by the stabilized atmosphere which

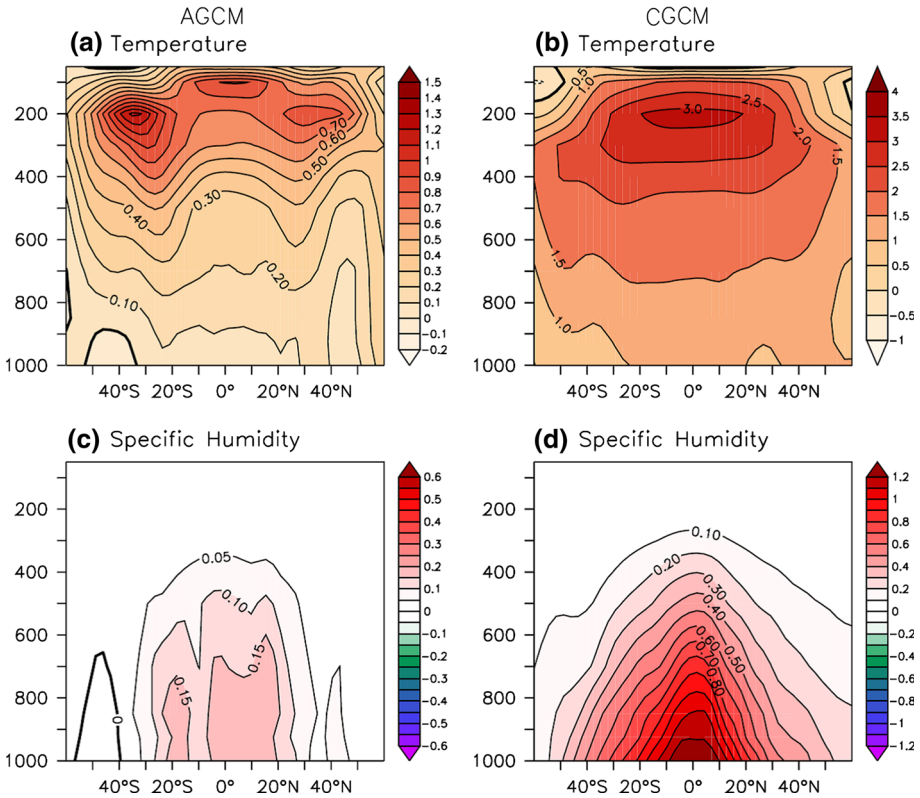

Fig. 9 Vertical profiles of zonally averaged temperature (°C) changes in response to the prescribed upper-tropospheric heating in **a** the AGCM (A-HEAT − A-CTRL) and **b** the CGCM (C-HEAT − C-CTRL) experiments. **c** and **d,** the corresponding specific humidity (g/kg) changes. 10-year means are used for AGCM experiments and 20-year means (the last 20 years of 50-year integrations) for CGCM experiments

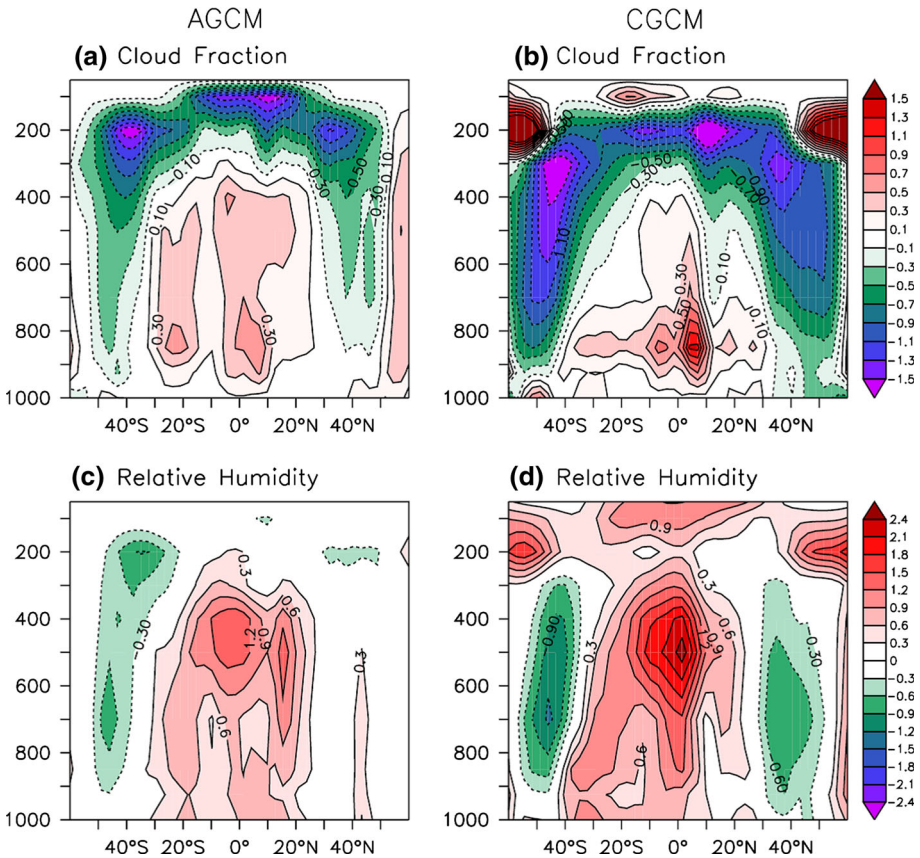

Fig. 10 Cloud fraction (%) changes due to the upper-tropospheric heating in **a** AGCM (A-HEAT − A-CTRL, *left column*) and **b** CGCM (C-HEAT − C-CTRL) experiments. **c** and **d** are the same but for relative humidity (%)

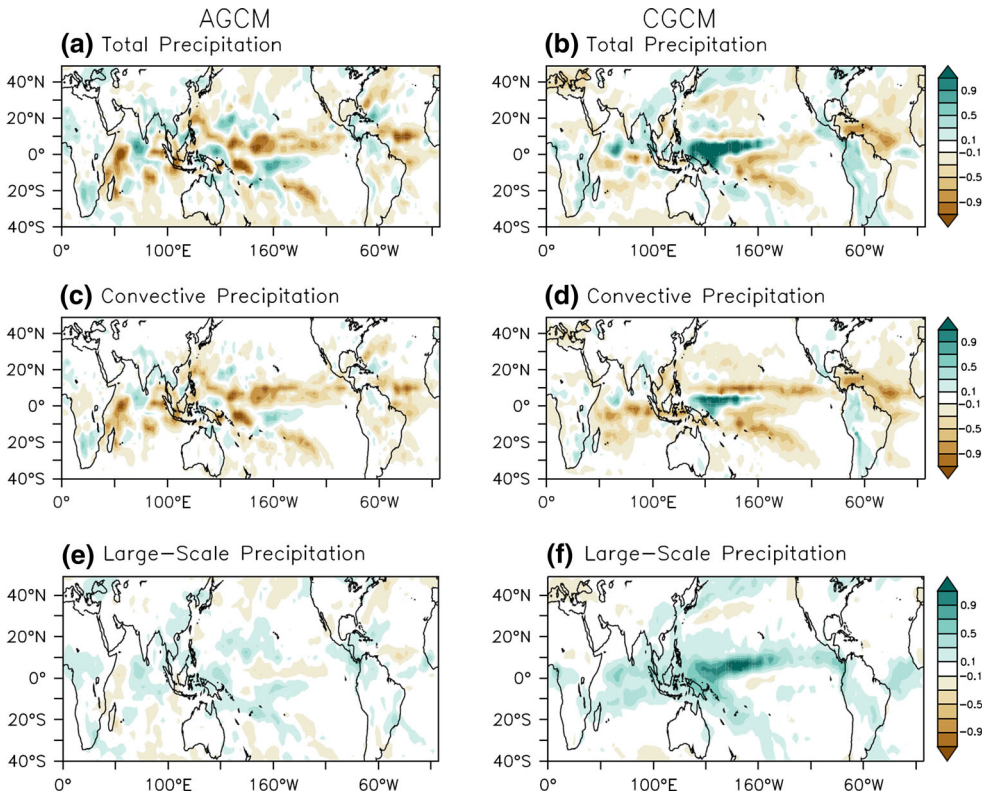

Fig. 11 Precipitation changes (mm/day) due to the upper-tropospheric heating in the AGCM (A-HEAT − A-CTRL, *left column*) and CGCM (C-HEAT − C-CTRL, *right column*) experiments: total rainfall (*upper row*), convective rainfall (*middle row*), and large-scale (non-convective) rainfall (*bottom row*)

increases the threshold for deep convection (Johnson and Xie 2010). Above results also imply that the precipitation decrease is larger than the evaporation decrease and this imbalance leads to an increase in moisture content in the atmosphere.

Note that the large-scale non-convective precipitation is intensified in most tropical regions (Fig. 11e), which facilitates increasing the mid- to lower-tropospheric temperature because of the latent heat release (Fig. 9a). Meanwhile, the intensified large-scale precipitation corresponds to the increased fraction of the mid- and low-level clouds (Fig. 10a), which tend to be more effective in reflecting shortwave radiation than high clouds so that the incoming shortwave radiation at the surface is reduced (Fig. 7b).

4.2 Understanding the role of the UTW–SST warming feedback in intensifying the initial sea surface warming

The above AGCM experiments well document how the UTW triggers the initial sea surface warming. However, the surface heat flux closely follows the SST changes in reality. Thus, an investigation of heat flux evolutions in the CGCM is instrumental for identifying the feedbacks which may amplify or dampen the initial SST warming over the tropical oceans. Considering the facts that heat flux plays the dominant role in shaping up the SST patterns near the tropics while ocean dynamics are important in regulating the SST patterns in the extratropics because of the difference in mean SST gradients (Xie et al. 2010), here we only focus on the heat flux changes averaged over the tropical oceans (30°S–30°N) (Fig. 12). As expected, the upward latent heat flux from the ocean to the atmosphere is substantially decreased in the first 2–3 years with its amplitude decreasing gradually afterwards accompanied by the steady sea surface warming. The decreased amplitude of the latent heat flux is caused by the competing effects between the increased atmospheric specific humidity and simultaneous rise of SST. By contrast, the downward longwave radiation at the ocean surface is increasing steadily and is mostly balanced by the decreasing incoming shortwave radiation. We claim that the increased longwave radiation largely reflects the contribution from the positive water vapor feedback (Bony et al. 2006; Soden and Held 2006). As a GHG, additional water vapor traps more downward longwave radiation and enhances the SST warming, which is, in turn, tied to moisture anomalies. The role of the positive water vapor feedback is further supported by the fact that the increasing rate of specific humidity is much larger in the CGCM experiments than the AGCM experiments (Fig. 9d vs. 9c).

The major processes by which the UTW (forced by either the GHGs or solar forcing) cause the sea surface warming can be summarized as the followings. With the GHGs or solar forcing, the atmosphere attains a rapid

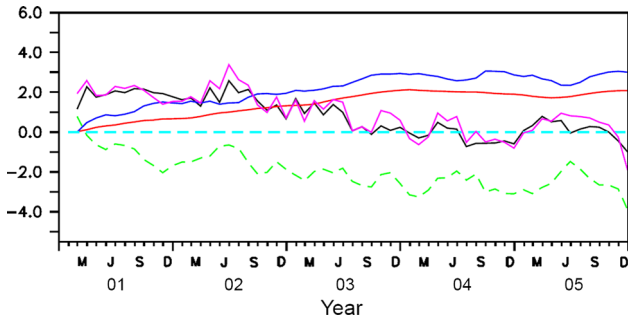

Fig. 12 The time evolution of the zonal (0°–360°) and meridional (30°S–30°N) average of SST (°C) and surface heat flux (W/m^2) changes in the first 5 years for the coupled model simulations associated with the upper-tropospheric heating (C-HEAT − C-CTRL): changes in SST multiplied by 3 (*red*), surface latent heat flux (*black*), shortwave radiation (*dashed green*), longwave radiation (*blue*) and the sum of above three heat fluxes (*pink*) at the surface. A 3-month running mean is applied, and five ensembles are used for the control and sensitivity experiments. Sensible heat flux change is neglected due to its small amplitude

response with stronger warming in the upper-troposphere than in the lower-troposphere. The UTW then suppresses surface wind speed and traps additional moisture in the lower-troposphere, thus reducing the surface upward latent heat flux but increasing downward longwave radiation to the ocean. As such, the SST becomes warmer and the positive water vapor feedback then further intensifies the SST warming via an increased downward longwave radiation. This is a slow process. The SST warming caused by the UTW can in turn feed back to intensify the initial UTW. In addition to the moist adiabatic adjustment process (Knutson and Manabe 1995; Manabe et al. 1965), the water vapor feedback may also contribute to strengthen the UTW as demonstrated by previous studies (Gettelman and Fu 2008; Minschwaner et al. 2006). The above two-way interaction completes a positive 'UTW–SST warming' feedback loop.

5 Summary and discussion

Future projections of climate changes by current climate models show a very robust feature characterized by more warming in the upper-troposphere than the lower-troposphere. Similarly, the fast response of the atmosphere to either GHGs or solar forcing also shows a maximum warming in the upper-troposphere over the tropical ocean areas. Improving the understanding of the impact of the fast UTW on the climate sensitivity is a challenging task because it is difficult to isolate its effects from that of other processes. In this study, we use prescribed upper-tropospheric heating experiments to address the potential role of UTW on sea surface warming by focusing on the surface energy budget. It is found that the UTW is able to increase water vapor in the lower-troposphere and suppress the surface wind speed, both contributing to trigger the initial SST warming by reducing the upward latent heat flux. The increase of water vapor also leads to more downward longwave radiation enhancing the sea surface warming. The sea surface warming can in turn feed back to intensify the UTW, completing a positive UTW–SST warming feedback.

To test the sensitivity of the SST response to the meridional heating profile, we make another coupled experiment (C-HEAT-30) by shifting the maximum heating to 30°S and 30°N (Fig. 13a). The vertical heating profile is the same as C-HEAT. The induced SST changes are characterized by a similar warming pattern with C-HEAT despite of weakened amplitude (Fig. 13b vs. 6a). Of particular interest is that a robust warming is seen over the equatorial region despite of the zero heating rate at the equator. In other words, the SST changes do not follow the meridional heating profile. How to understand this? We argue that the wave adjustment plays an important role in redistributing the UTW signal to the equatorial upper-troposphere which can further induce the tropical SST warming through the 'top-down' warming mechanism. With the involvement of the UTW–SST positive feedback, the equatorial SST and UTW can be both intensified. This argument is further corroborated by the vertical temperature changes pattern characterized by the maximum warming occurring in the equatorial upper-troposphere (Fig. 13c). Although the off-equatorial heating can also induce the tropical SST warming (Fig. 13), it should be noted that the equatorial upper-tropospheric heating is more efficient in driving the tropical SST warming demonstrated by a northward-shifted heating experiment (Xie et al. 2013).

Tropical tropospheric temperature and SST are coupled by the convections through moist adiabatic process. The physical process to achieve such a relation could be quite different depending on whether the initial warming is from the SST or from the troposphere. With an initial SST warming, the upper-troposphere tends to become warmer associated the convective adjustment. Given an initial UTW perturbation, it can alter the lower-tropospheric moisture and temperature so as to maintain the moist adiabatic lapse rate. The proposed 'top-down' warming mechanism is therefore viewed as one important part of the moist adiabatic adjustment. This also has some implication on understanding why it is difficult to destroy the moist adiabatic lapse rate in a convective-radiative equilibrium regime.

Global warming is the first order manifestation of increasing GHGs. This study establishes a 'top-down' warming mechanism, that is, the GHGs (or solar)-forced

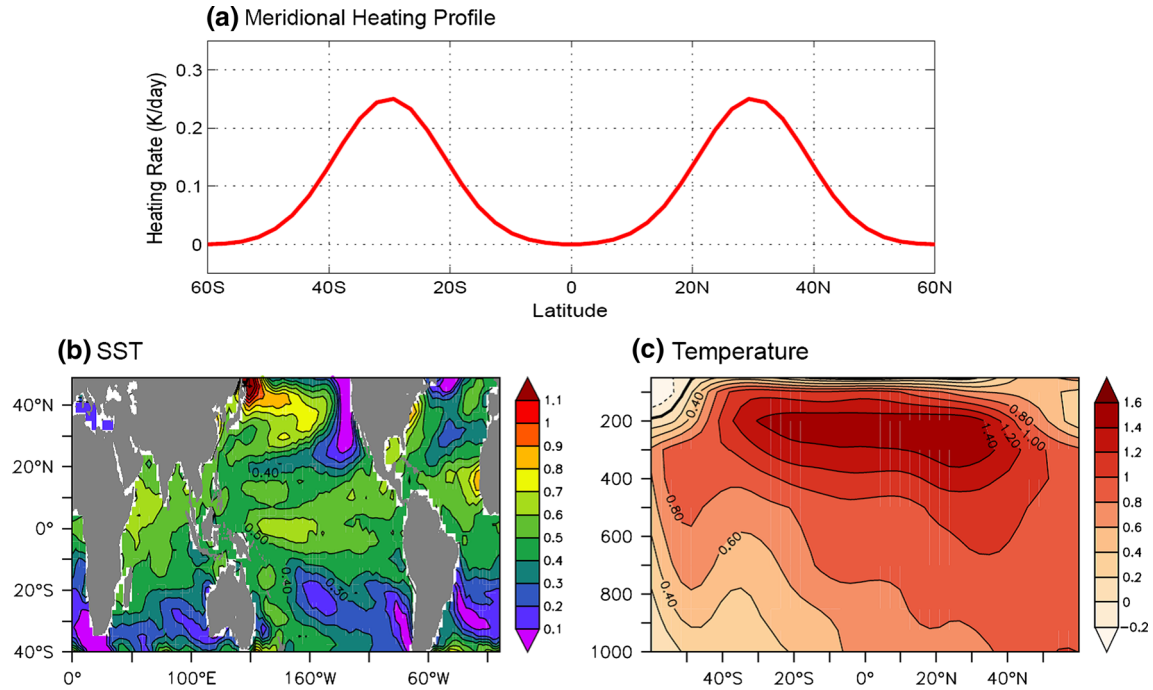

Fig. 13 Sensitivity experiment results with the maximum heating shifting to 30°S and 30°N and the heating rate is zero at the equator. **a** The meridional heating profile, **b** SST and **c** zonal (0°–360°) average of vertical temperature changes (C-HEAT-30 − C-CTRL). The vertical heating profile is the same as Fig. 4b

rapid UTW can further amplify the SST warming. The UTW can have important ramifications for the climate prediction problem and the understanding of the past and future changes of the clouds, precipitation and atmospheric circulations. For example, the changes in precipitation occur at a smaller increase rate than the moisture increase rate in projections of future climate by current start-of-the-art models (Held and Soden 2006). This fact has been attributed to weakened atmospheric circulation (Held and Soden 2006), the strong radiative constraints (Stephens and Ellis 2008; Takahashi 2009). The increased atmospheric stability associated with UTW may provide an alternative explanation for the less precipitation increase rate given the substantial reduction in deep convective precipitation in both the AGCM and the CGCM experiments (Fig. 11). A recent study by Liu et al. (2013) revealed that the solar-volcanic forcing can cause an intensified Walker circulation but the GHGs forcing weakens the Walker circulation given similar increase rate of global mean temperature; The solar forcing can also induce a stronger increase in precipitation than the GHGs forcing. The root cause was suggestively attributed to different impacts on the atmospheric stability (Liu et al. 2013). That is, the solar-volcanic forcing does not change the atmospheric stability but the GHGs forcing does which is likely due to the different responses of the temperature in the upper-troposphere.

This study is a general survey intended to shed light on the importance of the feedback between the UTW and sea surface warming, but it remains unclear how strong is this feedback. In other words, how much of the sea surface warming can be attributed to this feedback for the future projections? Considering the different impacts of the UTW on the convective and large-scale precipitation, the circulation changes are also expected to have different behaviors in the upper-troposphere and lower-troposphere. Further studies are required to address the above issues.

Acknowledgments The authors thank Shang-Ping Xie, Qiang Fu, Tim Li and three anonymous reviewers for their valuable comments. This study is supported by the International Pacific Research Center which is funded jointly by JAMSTEC, NOAA, and NASA. B.X., B.W. and J.Y.L. acknowledge APEC Climate Center (APCC) and Global Research Laboratory (GRL) grant funded by the Ministry of Education, Science and Technology (MEST 2011-0021927). J.Y.L. is supported by the MEST Brain Pool program. We acknowledge the World Climate Research Programme's Working Group on Coupled Modeling, which is responsible for CMIP, and we thank the climate modeling groups for producing and making available their model output.

References

Andrews T, Forster PM, Gregory JM (2009) A surface energy perspective on climate change. J Clim 22:2557–2570

Bala G, Caldeira K, Nemani R (2010) Fast versus slow response in climate change: implications for the global hydrological cycle. Clim Dyn 35:423–434

Bony S et al (2006) How well do we understand and evaluate climate change feedback processes? J Clim 19:3445–3482

Butler AH, Thompson DWJ, Heikes R (2010) The steady-state atmospheric circulation response to climate change-like thermal forcings in a simple general circulation model. J Clim 23: 3474–3496

Cao L, Bala G, Caldeira K (2012) Climate response to changes in atmospheric carbon dioxide and solar irradiance on the time scale of days to weeks. Environ Res Lett 7. doi:10.1088/1748-9326/7/3/034015

Collins WD et al (2006) Radiative forcing by well-mixed greenhouse gases: estimates from climate models in the Intergovernmental Panel on Climate Change (IPCC) Fourth Assessment Report (AR4). J Geophys Res 111:D14317

Colman RA (2001) On the vertical extent of atmospheric feedbacks. Clim Dyn 17:391–405

Dong B, Gregory JM, Sutton RT (2009) Understanding land–sea warming contrast in response to increasing greenhouse gases. Part I: transient adjustment. J Clim 22:3079–3097

Easterling D, Meehl GA, Parmesan C, Changnon SA, Karl TR, Mearns LO (2000) Climate extremes: observations, modeling, and impacts. Sci 289:2068–2074

Frierson DMW, Lu J, Chen G (2007) Width of the Hadley cell in simple and comprehensive general circulation models. Geophys Res Lett 34:L18804

Fu Q, Manabe S, Johanson CM (2011) On the warming in the tropical upper troposphere: models versus observations. Geophys Res Lett 38:L15704

Gettelman A, Fu Q (2008) Observed and simulated upper-tropospheric water vapor feedback. J Clim 21:3282–3289

Gregory JM, Forster PM (2008) Transient climate response estimated from radiative forcing and observed temperature change. J Geophys Res 113:D23105

Hansen J, Sato M, Ruedy R (1997) Radiative forcing and climate response. J Geophys Res 102:6831–6864

Held IM, Soden BJ (2006) Robust responses of the hydrological cycle to global warming. J Clim 19:5686–5699

Johnson NC, Xie S-P (2010) Changes in the sea surface temperature threshold for tropical convection. Nat Geosci 3:842–845

Kamae Y, Watanabe M (2012) Tropospheric adjustment to increasing CO_2: its timescale and the role of land–sea contrast. Clim Dyn. doi:10.1007/s00382-012-1555-1

Knutson TR, Manabe S (1995) Time-mean response over the tropical pacific to increased C02 in a coupled ocean–atmosphere model. J Clim 8:2181–2199

Lee J-Y, Wang B (2013) Future change of global monsoon in the CMIP5. Clim Dyn. doi:10.1007/s00382-012-1564-0

Liu J, Wang B, Cane MA, Yim S-Y, Lee J-Y (2013) Divergent global precipitation changes induced by natural versus anthropogenic forcing. Nature 493:656–659

Lu J, Vecchi GA, Reichler T (2007) Expansion of the Hadley cell under global warming. Geophys Res Lett 34:L06805

Ma J, Xie S-P, Kosaka Y (2011) Mechanisms for tropical tropospheric circulation change in response to global warming. J Clim 25:2979–2994

Manabe S, Smagorinsky J, Strickler RF (1965) Simulated climatology of a general circulation model with a hydrologic cycle. Mon Weather Rev 93:769–798

Meehl GA et al (2007) Global climate projections. In: Solomon S et al (eds) Climate change 2007: the physical science basis. Cambridge University Press, Cambridge

Minschwaner K, Dessler AE, Sawaengphokhai P (2006) Multimodel analysis of the water vapor feedback in the tropical upper troposphere. J Clim 19:5455–5464

Mitchell JFB (1983) The seasonal response of a general circulation model to changes in CO_2 and sea temperatures. QJR Meteorol Soc 109:113–152

Richter I, Xie S-P (2008) Muted precipitation increase in global warming simulations: a surface evaporation perspective. J Geophys Res 113:D24118

Roeckner E et al (1996) The atmospheric general circulation model ECHAM-4: model description and simulation of present-day climate. Max-Planck-Institut für Meteorologie Rep 218, Hamburg, Germany, p 90

Santer BD et al (2008) Consistency of modelled and observed temperature trends in the tropical troposphere. Int J Climatol 28:1703–1722

Schneider T, O'Gorman PA, Levine XJ (2010) Water vapor and the dynamics of climate changes. Rev Geophys 48:RG3001

Sobel AH, Nilsson J, Polvani LM (2001) The weak temperature gradient approximation and balanced tropical moisture waves. J Atmos Sci 58:3650–3665

Soden BJ, Held IM (2006) An assessment of climate feedbacks in coupled ocean–atmosphere models. J Clim 19:3354–3360

Solomon S (2007) Climate change 2007: the physical science basis. Cambridge University Press for the Intergovernmental Panel on Climate Change, Cambridge

Stephens GL, Ellis TD (2008) Controls of global-mean precipitation increases in global warming GCM experiments. J Clim 21:6141–6155

Takahashi K (2009) Radiative constraints on the hydrological cycle in an idealized radiative–convective equilibrium model. J Atmos Sci 66:77–91

Taylor KE, Stouffer RJ, Meehl GA (2011) An overview of CMIP5 and the experiment design. Bull Am Meteorol Soc 93:485–498

Wang S, Gerber EP, Polvani LM (2012) Abrupt circulation responses to tropical upper-tropospheric warming in a relatively simple stratosphere-resolving AGCM. J Clim 25:4097–4115

Wang B, Xiang B, Lee J-Y (2013) Subtropical high predictability establishes a promising way for monsoon and tropical storm predictions. PNAS. doi:10.1073/pnas.1214626110

Xiang B, Wang B (2013) Mechanisms for the advanced Asian Summer Monsoon onset since the mid-to-late 1990s. J Clim 26:1993–2009

Xiang B, Wang B, Ding Q, Jin FF, Fu X, Kim H-J (2012) Reduction of the thermocline feedback associated with mean SST bias in ENSO simulation. Clim Dyn 39:1413–1430

Xie S-P, Deser C, Vecchi GA, Ma J, Teng H, Wittenberg AT (2010) Global warming pattern formation: sea surface temperature and rainfall. J Clim 23:966–986

Xie S-P, Lu B, Xiang B (2013) Similar spatial patterns of climate responses to aerosol and greenhouse gas changes. Nature Geosci (in press)

Yin JH (2005) A consistent poleward shift of the storm tracks in simulations of 21st century climate. Geophys Res Lett 32:L18701